Materials Research Bulletin 94 (2017) 164–169

Contents lists available at ScienceDirect

Materials Research Bulletin

journal homepage: www.elsevier.com/locate/matresbu

Influence of selenization atmosphere on the $Cu_2ZnSn(S,Se)_4$ thin films and its correlation to the performance of solar cells

Guilin Chen[a,b,*,1], Weihuang Wang[a,1], Biyun Zhang[a], Shuiyuan Chen[a,b,*], Zhigao Huang[a,b], Bin Zhuang[a,b]

[a] Fujian Provincial Key Laboratory of Quantum Manipulation and New Energy Materials, College of Physics and Energy, Fujian Normal University, Fuzhou 350007, China

[b] Fujian Provincial Collaborative Innovation Center for Optoelectronic Semiconductors and Efficient Devices, Xiamen, 361005, China

ARTICLE INFO

Article history:
Received 1 February 2017
Received in revised form 27 May 2017
Accepted 28 May 2017
Available online 4 June 2017

Keywords:
$Cu_2ZnSnS_xSe_{4-x}$
Thin films
Selenization
Atmosphere

ABSTRACT

Selenization is a key process to prepare $Cu_2ZnSnS_xSe_{4-x}$ (CZTSSe) thin films from sulfide for high efficient solar cell. To explore the effect of annealing atmosphere on the substitution of S by Se in Cu_2ZnSnS_4 (CZTS) thin films, different selenization atmosphere (Vacuum or Ar) are used. By examining the annealed sample, it is found that selenization under Ar atmosphere replaces S with Se more efficiently, resulting large grain and small band-gap. The reaction kinetics has been studied to explore such phenomena. It demonstrates that the substitution reaction is enhanced when the flowing Ar carries off S gas. Finally, the effect of annealing atmosphere on oxide-based CZTSSe devices has also been studied. The Vacuum selenized CZTSSe device shows a higher efficiency of 4.4%, due to the more appropriate band-gap. To the best of our knowledge, this is the best device performance in oxides nanoparticles-derived CZTSSe solar cell.

1. Introduction

Recently, $Cu_2ZnSn(S,Se)_4$ (CZTSSe)-based material have attracted extensive attention as sustainable alternatives to Cu(In, Ga)Se_2 (CIGS) for solar cells, as it has suitable optical and electronic properties [1,2]. Up to now, the highest power conversion efficiency of 12.6% has been achieved from the Se-contained CZTSSe thin films, which is higher compared with the efficiencies of the Se-free Cu_2ZnSnS_4 (CZTS) thin films solar cell [3]. It can be explained as follow: Se-contained CZTSSe displays (1) shallower energy levels and less bulk defect density; (2) longer minority carrier diffusion lengths; (3) good crystalline, comparing with CZTS.

The most common route to prepare mixed sulfoselenide CZTSSe is selenization of sulfide (including quaternary CZTS, blended binary/ternary, binary sulfide or other sulfur contained precursor) under Se vapor ambient. For example, IBM has reported the best performing CZTSSe device with an efficiency of 12.6% by selenization of hydrazine-based binary sulfide precursor [3]. CZTSSe thin film fabricated through selenizing binary and ternary nanoparticles under Se vapor resulted in efficiency of up to 9.6%, while those using CZTS nanocrystals yielded an efficiency of 7.2% [4,5]. Furthermore, Schnabel et al. also has demonstrated a 7.5% efficient CZTSSe device by selenization of metal salts precursor dissolved in DMSO (Dimethyl Sulfoxide) [6]. During those annealing process, the replacement of small atom S by bigger atom Se can assist the grain growth and densification for high quality CZTSSe thin films. So proper selenization condition plays a crucial role in growing CZTSSe absorbers. The effect of selenization condition (e.g. temperature, soaking time, etc.) on CZTSSe thin films have been researched widely. For instance, Carrete et al. [7] have explored the effect of selenization on the properties of spray deposited CZTSSe thin films using different temperatures (475–575 °C). Both Embden [8] and Singh [9] have reported the influence of the selenization time on the grain growth of the CZTSSe thin films by controlling the substitution of S by Se.

Another important selenization condition is the annealing atmosphere, which will control the transport kinetics of Se vapor from Se powder to precursor thin films. Typically, selenization is conducted either in vacuum or under inert gas atmosphere to grow CZTSSe. Wang et al. [10] have fabricated a CZTSSe thin film by selenizing precursor in sealed tube under vacuum atmosphere.

* Corresponding authors.
E-mail addresses: glchen@fjnu.edu.cn (G. Chen), sychen@fjnu.edu.cn (S. Chen).
[1] These authors contributed equally to this work and should be considered co-first author.

http://dx.doi.org/10.1016/j.materresbull.2017.05.053
0025-5408/

While Wooseok et al. [11] have prepared CZTSSe thin films by selenizing CZTS using selenium pellets under Ar flowing, which resulted a 4.1% efficient CZTSSe device. Chu et al. [12] have also revealed that the control of nitrogen pressure can change Se supply during the preparation of CZTSSe thin films. Although so many researches reported the selenization may be carried out in either vacuum or inert gas atmosphere, the comparing study on the effects of selenization atmosphere on the substitution of S by Se in CZTS thin films were conducted rarely. The influence mechanism is not yet well understood.

In this paper, a two-step annealing process was involved after coating oxide nanoparticles on a glass substrate: the first process for converting of oxide into CZTS by sulfurization; the second substitution process for grain growth and densification in the CZTSSe film by selenization. In order to explore the effect of selenization atmosphere on the CZTSSe thin films, two selenization types (Vacuum or Ar atmosphere) has been executed using elemental selenium vapor. The influence of selenization atmosphere on the structure, morphology and band-gap of CZTSSe was studied carefully. Meanwhile, the corresponding devices were fabricated to check such effect.

2. Experimental

The CZTSSe thin films were prepared by sequential sulfurization and selenization of oxides precursor. First, the oxides precursor thin films (Cu:Zn:Sn = 2:1:1) were coated by doctor blade, as described previously [13]. Secondly, the CZTS thin films (denoted as "S" in the figure) were obtained by vacuum sulfurization (base $\sim 10^{-1}$Pa) of oxide layers, which was carried out at 550 °C for 30 min using solid sulfur. Finally, selenization of the resulted CZTS thin film was conducted using Se pellets as a source of Se vapor either in vacuum (base P $\sim 10^{-3}$ Pa) or under flowing Ar (20 sccm) at atmospheric pressure. As vacuum selenization was operated, both sample and Se pellets were sealed in quartz ampoules together (also called "close" system, denoted as "V-Se" in the figure). Another typical annealing atmosphere is Ar-selenization, where the Se vapor was transported to the CZTS thin films by the flowing Ar (also called "open" system, denoted as "Ar-Se" in the figure). The same temperature and time for Vacuum and Ar selenization were fixed as follows: selenization temperature was 550 °C, while selenization time was 30 min. The ramp rate was 50 K/min.

To make the devices, the CZTS and CZTSSe thin films were first deposited on Mo-coated glass substrate. A CdS buffer layer was then deposited on CZTS and CZTSSe thin films by chemical bath deposition. Sequentially, 50 nm/400 nm thick i-ZnO/ZnO:Al transparent conducting layer were prepared by sputtering. Finally, silver paint was deposited as the top electrode. Previous reports have proven that the Cu-poor and Zn-rich composition of CZTS and CZTSSe devices showed higher efficiency, because a Zn-rich content can suppress the formation of shallow acceptors (Cu_{Zn}) [14]. So the CZTS and CZTSSe thin films for devices were designed to have compositions of Cu/(Zn + Sn) = 0.8 and Zn/Sn = 1.2 in this work.

The crystal structure of the sample was identified by X-ray diffraction (XRD) method (CuKα, λ = 1.54178 Å). The field emission scanning electron microscope (SEM, JSM-6700F) was used to observe the morphology of the thin films. The component was determined by Energy dispersive X-ray Spectroscopy (EDX). The Raman tests were performed using a LABRAM-HR micro-Raman system with a laser source of 532 nm. To study the chemistry nature of CZTS and CZTSSe thin films, the X-ray photoelectron spectroscopy (XPS) spectra were executed out (thermo ESCALAB 250). The optical absorption spectrum was measured using a UV-vis-365-type spectrophotometer. The photoelectric conversion efficiency (PCE) of the devices was tested under standard AM1.5 conditions (100 mW/cm^2; 25 °C). The external quantum efficiency (EQE) of devices was characterized using an incident PCE measurement unit (PV measurement, Inc., USA).

3. Results and discussions

Table 1 shows the EDX results of CZTS and CZTSSe thin films. For all the samples, the Cu/Zn/Sn ratios (also expressed as Cu/(Zn + Sn), Zn/Sn) are nearly equal to the composition of the initial material (Cu:Zn:Sn = 2:1:1), indicating that metal elements ratios are controllable during the deposition of both CZTS, Vacuum selenized CZTSSe and Ar selenized CZTSSe. This is due to the relatively high stability of oxide precursor, as discussed previously [13]. Table 1 also shows the selenized CZTS thin films under various atmosphere have different S and Se content. It was found that selenium content reached 26.9% when the CZTS thin films suffered from Vacuum selenization. The Se/S ratio is about 26.90/22.13, showing a moderate Se content in V-Se CZTSSe sample. In contrast, the Ar selenized CZTSSe film exhibited sulfur content of 2.25%. It demonstrated that almost 95% of sulfur in CZTS thin film was replaced by selenium under Ar selenization. The increase of Se contents is related to the more effective incorporation of Se into CZTS under Ar selenization, comparing with vacuum selenization. Therefore, using different annealing atmosphere is a feasible approach to grow CZTSSe thin films with Se/S ratio control.

To examine the phase purity of the sulfurized and post-selenized films, XRD test was carried out, as shown in Fig. 1. After sulfurization of oxide precursor, the thin film appears almost pure CZTS phase (see JCPDS 26-0575) [15]. Once the selenization was implemented in the resulted CZTS thin films, the entire diffraction peaks shift from CZTS to $Cu_2ZnSnSe_4$ (CZTSe) (JCPDS 52-0868) as S atom was replaced by Se atom [16]. It was absent of structure change or secondary phases during the substitution. Fig. 1(b) shows the magnified view of XRD peak corresponding to (112) plane. As the Vacuum-selenization was used, the XRD peaks shift to the left slightly. Because the replacement of small atom S by big atom Se will expand the unit cell volume. When Ar-selenization was introduced, a distinct shift of the (112) XRD peak towards lower angles is observed, suggesting tendency of the incorporation of selenide into CZTS thin films is stronger. In the case of Ar-selenized CZTSSe sample, a tiny shift of the XRD peak to higher angles is observed, referring CZTSe (JCPDS 52-0868), which demonstrates the presence of small amount of residual sulfur in

Table 1
Compositions of precursor and CZTS(e) films as measured using EDX.

	Cu (at%)	Zn (at%)	Sn (at%)	S (at%)	Se (at%)	Cu/(Zn + Sn)	Zn/Sn
Starting Material	50.00	25.00	25.00	–	–	1	1
Precursor	16.88	8.37	8.50	–	–	1.00	0.98
CZTS	25.52	12.43	12.75	49.31	–	1.01	0.97
CZTS-V-Se	25.97	12.68	12.33	22.13	26.90	1.03	1.02
CZTS-Ar-Se	25.32	12.89	12.20	2.25	47.34	1.01	1.05

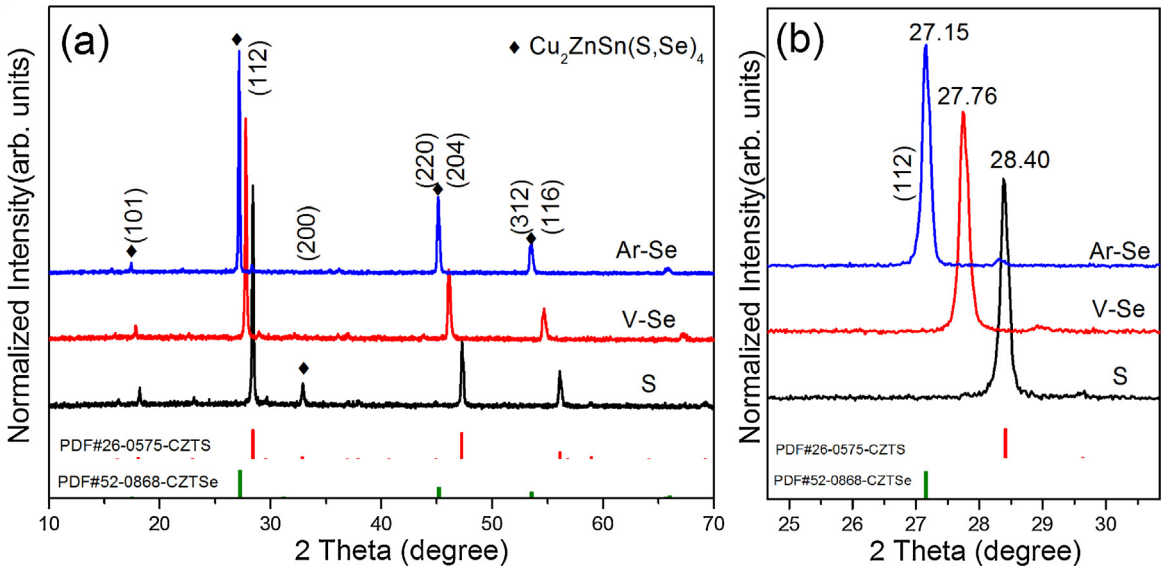

Fig. 1. The XRD patterns of CZTS and post selenized CZTSSe thin films.

the lattice. So selenization under Ar atmosphere is more effective to replace sulfur in CZTS by selenium than vacuum selenization.

Simple XRD measurement, however, cannot determine clearly whether CZTS or CZTSSe films are pure phase, since the possible secondary phase, such as $Cu_2SnS(e)_3$ and ZnS(e) adopt an analogous zinc-blende-related structure. So the peaks of $Cu_2SnS(e)_3$ and ZnS(e) may overlap with the XRD pattern of CZTS and CZTSSe thin films. Raman can distinguish CZTS/CZTSSe and possible secondary phase easily. Fig. 2(a) shows the Raman spectra of the CZTS and CZTSSe thin films. As the oxides thin films were sulfurized at high temperature, the annealed films appear the main modes at around 287 and 337 cm^{-1} which were assigned to CZTS [17,18]. After Vacuum selenization of CZTS thin films, the film shows two-mode A1 behavior at ~215 cm^{-1} (CZTSe) and at ~329 cm^{-1} (CZTS) which can be assigned to A1 Se–Se and A1 S–S vibrations in CZTSSe respectively [19,20]. Comparing with pure A1 Se–Se of CZTSe and A1 S-S CZTS, an obvious shift of the A1 Se–Se and A1 S–S Raman scattering towards one other is demonstrated in Vacuum selenized CZTSSe thin film, following the same trend as

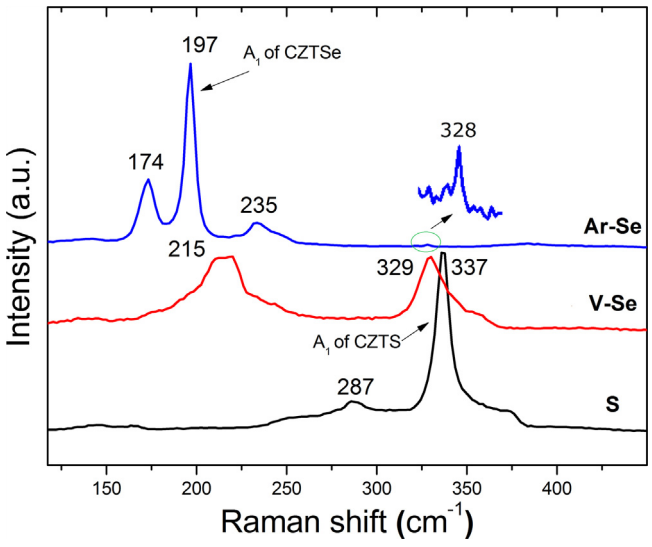

Fig. 2. The Raman of CZTS and post selenized CZTSSe thin films.

previously reported for CZTSSe with an moderate S/Se ratio [21–23]. The ratios of peak intensity of A1 Se–Se and A1 S–S is intermediate, which is due to the fact that Se/S ratio keeps dynamic equilibrium under Vacuum selenization ("close" system). As the Ar selenization was used, the Raman peak of A1 Se–Se vibration in CZTSSe shifts to ~197 cm^{-1}, which is close to that of pure CZTSe. Meanwhile, the small Raman peak of A1 S–S vibration is barely detectable at 329 cm^{-1}. It manifested that only small amount of residual sulfur existed in the Ar-selenized CZTSSe, which is in agreement with the EDX and XRD results. The XPS analysis also confirmed the coexistence of S and Se in V-Se CZTSSe, while little sulfur survives in Ar-Se CZTSSe (Fig. S1). In short, the selenization atmosphere can affect the incorporation of Se into CZTS significantly.

The SEM micrographs of the CZTS and CZTSSe thin films selenized under Vacuum or Ar atmosphere were shown in Fig. 3. The sulfurized CZTS thin films were composed of non-uniform small grain size, which will lead to defects and then deteriorate the device performance. As the CZTS thin films suffered from Vacuum selenization, the grain size increased mildly. When the Ar-selenization was introduced, it was observed that individual nanoparticles were merged into a larger one, resulting a densely packed, compact and uniform morphology. Cross-section also exhibits a smooth surface. Such a uniform dense structure with large grain is comparable with those produced by the vacuum or hydrazine based method. So both Vacuum and Ar selenization can assist the grain growth of CZTSSe thin films, which will improve the efficiency of polycrystalline solar cells. However, the grain size of annealed CZTSSe thin films was also affected by the selenization atmosphere. From the point of morphology of CZTSSe thin films, the Ar-selenized CZTSSe thin films with very large grain seem to been more suitable for high efficient CZTSSe thin films solar cell.

On the basis of the above results, it can be seen that the evaporation of Se under different atmosphere lead to CZTSSe thin films with distinct properties. Comparing with the Vacuum selenization, the Ar-selenized CZTSSe exhibits better crystalline and larger grain size, demonstrating the more effective selenization. Regarding that sulfurized CZTS thin films in this work have nearly stoichiometric composition, the growth of CZTSSe thin films cannot be caused by the well known liquid CuSe assisted growth [24]. Rather Se itself may act as a medium of growth by enhancing

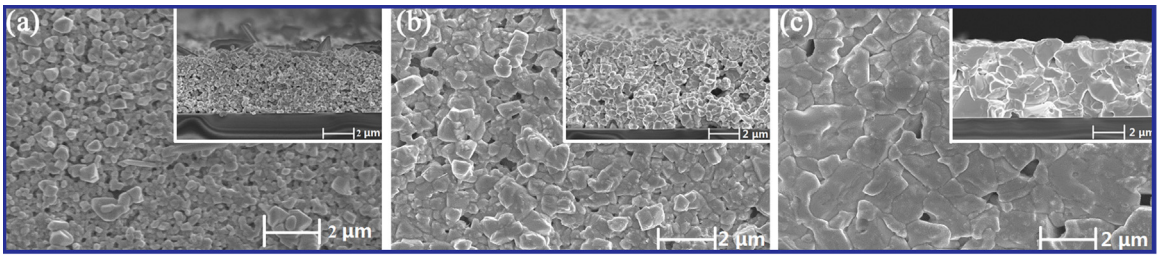

Fig. 3. SEM of the (a) CZTS thin film, (b) Vacuum selenized CZTSSe thin films, (c) Ar selenized CZTSSe thin films.

the diffusion of constituents. One possible explain is that the better crystalline in Ar-selenized CZTSSe thin films can be caused by the higher Se vapor pressure under Ar atmosphere, which is similar to the case of CIGSe growth [25]. Another possible explains is that the selenization atmosphere directly controls the kinetics of Se vapor from solid Se to sample. It can be inferred from the chemical reactions occurred during the selenization process as follows:

$$Cu_2ZnSnS_4 + xSe_m(g) \rightarrow Cu_2ZnSn(Se,S)_4 + yS_n(g)$$

In the case of Ar selenization, Ar gas carry more Se to CZTS thin films, then more and more sulfur in CZTS was replaced by Se. Meanwhile, the product of S from CZTS will be taken away in such an "open" system, and the selenization reaction will be accelerated, as shown in the schematic diagram (Fig. 4). However, the incorporation of Se reached a kinetic balance under the Vacuum selenization ("close" system) at last. This steady state equilibrium in Vacuum selenization is similar to the effect of annealing time, in which the S/Se ratio almost stays constant with increase in annealing time [26]. Therefore, the annealing atmosphere plays an important role on the growth of CZTSSe thin films.

From the above analysis, it was found that the selenization atmosphere affects the structure, morphology and optical properties of CZTSSe thin films significantly. To study the effect of various properties of as prepared CZTSSe thin films on the corresponding device performance, the light and dark J–V measurements were conducted, as shown in Fig. 5(a–c). The detailed parameters of each device were enclosed in the figure. As can be seen, the CZTS, Vacuum-selenized CZTSSe and Ar-selenized CZTSSe solar cell exhibited efficiency of 3.08, 4.4% and 3.4% without anti-reflection layer respectively. Regardless of selenization atmosphere, the PCE of CZTSSe devices were higher than that of pure sulfur CZTS device. It may be due to the shallower energy levels, less bulk defect density, longer minority carrier diffusion lengths and good crystalline for the Se-contained CZTSSe thin films. On the other hand, although Ar-selenized CZTSSe thin film shows a larger grain size than Vacuum-selenized CZTSSe thin film, the PCE of Vacuum-selenized CZTSSe device is still higher than that of Ar-selenized CZTSSe device. Because the Ar-Se CZTSSe have a more suitable band gap of 1.2 eV, which is close to that of the current CZTSSe champion device [3]. This demonstrates the strong correlation between band gap of CZTSSe film and device performance. So the band gap dependence of short circuit current density (Jsc) and open circuit voltage (Voc) were plotted in Fig. 5(d, e). The gray dotted lines in the figures can be used as eye guides, showing some correlations. The max Jsc was introduced to examine the changed tend of Jsc, which was calculated from solar spectrum (Fig. 5d). There is similar rising amplitude for Jsc and max Jsc as the band gap decreases, because of the increasing light absorption. In contrast, the Voc shows an opposite trend (Fig. 5e). This increasing in Voc is caused by larger band gap. It must also be mentioned that Voc deficit decrease as the Se incorporated into CZTS, which may be due to the decrease of Fermi level pinning, band tails and bulk defects [27–29]. Consequently, the substitution of S by Se raises the Jsc on the cost of decreased the Voc, which lead to max Jsc × Voc values in Vacuum-selenized CZTSSe devices. To the best of our knowledge, this efficiency of V-Se CZTSSe device is higher than the previously-reported solar cells based on oxide nanoparticels derived CZTS-based devices [13]. However, this efficiency is still lower than that of current CZTSSe champion devices [3]. To elucidate the origin of this gap, the J-V curves were redraw according to the Sites' method [30], as shown in Fig. 5(f, g). The diode parameters, such as series resistance (Rs), diode ideality factor (n) and reverse saturation current density (J_0) were extracted. The relative high Rs, n as well as J_0 for all the devices were observed, which is responsible for the low PCE. The cross-over features of light and dark J–V indicated a non-ideal *p-n* junction property again. It is also noticed that the higher Rs in pure sulfur CZTS may be attributed partly to small grain size of CZTS. On the other hand, the square resistance of AZO in our devices is as high as 50 Ω/□, which also enlarges Rs of device. So the

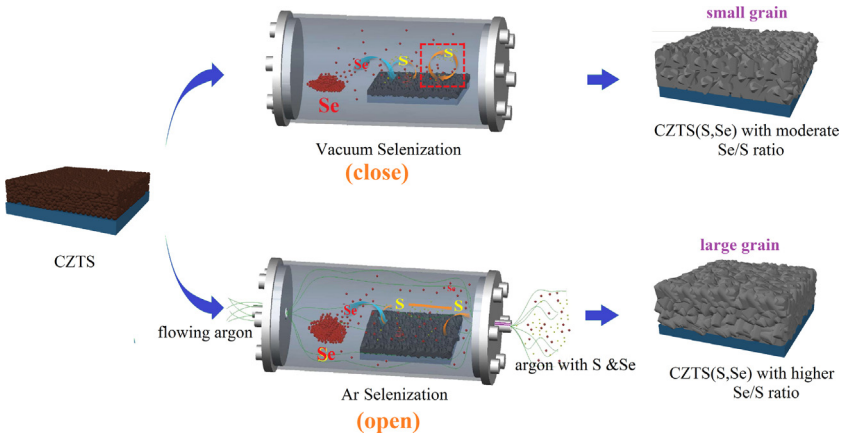

Fig. 4. The schematic diagram of selenization under Vacuum or Ar atmopshere.

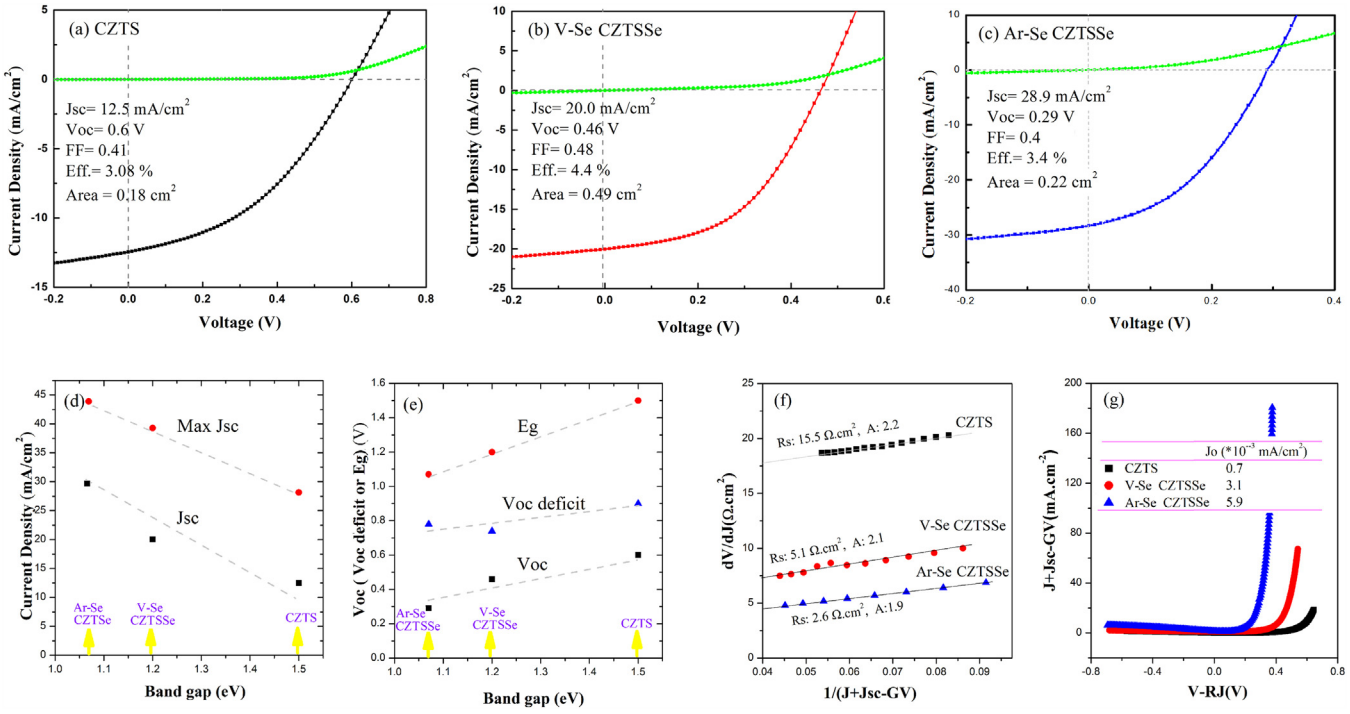

Fig. 5. Light and dark J–V characteristics of (a) CZTS, (b) Vacuum-selenized CZTSSe and (c) Ar-selenized CZTSSe solar cell. (d) Jsc and Jmax; (e) Voc and Voc deficit with varying band gap value; (f) R–J curves (g) ln(J + Jsc) with fit used to determine Rs, A and J_0 for the as-prepared TFSC.

optimization of device fabrication process is ongoing to improve the device efficiency.

Fig. 6 shows the EQE curve of the CZTS, Vacuum-selenized CZTSSe and Ar-selenized CZTSSe thin film solar cells. The EQE losses in the range of 300 ~ 550 nm is ascribed to CdS and i-ZnO/AZO layer absorption. For wavelengths higher than 550 nm, the as prepared absorber layers have various cut-off absorption edge. The band gap of CZTS, Vacuum-selenized CZTSSe and Ar-selenized CZTSe absorber layers determined from the cut-off wavelength EQE curve using linear extrapolation are 1.53, 1.18 and 1.09 eV respectively, which are consistent with the value obtained from the above UV–vis spectroscopy analysis (Fig. S2). The integrated current from EQE are about 29.6 mA/cm^2, 20 mA/cm^2 and 12.5 mA/cm^2 for Ar-selenized CZTSe, Vacuum-selenized CZTSSe and CZTS devices, which agree well with the Jsc from J-V curve. It can also see that Jsc increases strongly with the decrease of the band gap, because a broader absorption allows more photons to be absorbed. From the J-V and EQE analysis, the efficiency is found to be still limited by several factors, however, the results are encouraging. As the oxide nanoparticles-based method has been successfully applied in CIGS solar cell, it is also suggested that such a low cost route could fabricate CZTSSe devices as good as the CIGS devices. This can be expected by optimizing the process of devices fabrication in the future.

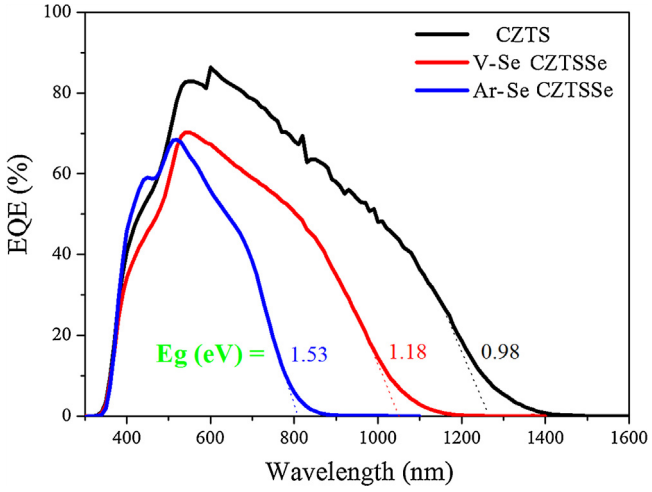

Fig. 6. (a) Quantum efficiency curve of the CZTS, Vacuum-selenized CZTSSe and Ar – selenized CZTSSe solar cell.

4. Conclusion

In summary, CZTSSe thin films have been prepared by selenization of pre-sulfurized CZTS thin films under Vacuum or Ar atmosphere. The effects of selenization atmosphere on the properties of oxide derived CZTSSe thin films were investigated. It revealed that Ar selenizaiton have higher Se supply to CZTS through carrier gas, meanwhile the substitution was accelerated by carried off S gas, which has be explained by selenization reaction kinetics. The resulted Ar-selenized CZTSSe thin films show larger grains size, while the Vacuum-selenized CZTSSe thin films have more suitable band gap. Finally, the Vacuum selenized CZTSSe device Exhibits 4.4% efficiency with a Jsc of 20 mA/cm^2, Voc of 0.46 V, and FF of 48% (AM 1.5 G, 100 mW/cm^2), which is the highest efficiency thus far reported for oxide nanoparticles-derived CZTSSe thin film solar cells. It is expected to improve performance of CZTSSe device in the future by optimizing the device fabrication process.

Acknowledgment

This work was supported by National Natural Science Foundation of China (Grant No. 51502037), Natural Science Foundation of Fujian Province, China (Grant No. 2015J05096).

Appendix A. Supplementary data

Supplementary data associated with this article can be found, in the online version, at 10.1016/j.materresbull.2017.05.053.

References

[1] J.B. Li, V. Chawla, B.M. Clemens, Adv. Mater. 24 (2012) 720–72.
[2] N.M. Shinde, D.P. Dubal, D.S. Dhawale, C.D. Lokhande, J.H. Kim, J.H. Moon, Mater. Res. Bull. 47 (2012) 302–307.
[3] W. Wang, M.T. Winkler, O. Gunawan, T. Gokmen, T.K. Todorov, Y. Zhu, D.B. Mitzi, Adv. Energy Mater. 4 (2014) 403–410.
[4] Y. Cao, M.S. Denny, J.J.V. Caspar, W.E. Farneth, Q. Guo, A.S. Ionkin, L.K. Johnson, M. Lu, I. Malajovich, D. Radu, H.D. Rosenfeld, K.R. Choudhury, W. Wu, J. Am. Chem. Soc. 134 (2012) 15644–15647.
[5] Q. Guo, G.M. Ford, W.C. Yang, B.C. Walker, E.A. Stach, H.W. Hillhouse, R. Agrawal, J. Am. Chem. Soc. 132 (2010) 17384–17386.
[6] T. Schnabel, M. Low, E. Ahlswede, Sol. Energy Mater Sol. Cells 117 (2013) 324–328.
[7] A. Carrete, A. Shavel, X. Fontane, J. Montserrat, J. Fan, M. Ibáñez, E. Saucedo, A. Pérez-Rodríguez, A. Cabot, J. Am. Chem. Soc. 135 (2013) 15982–15985.
[8] J.v. Embden, J. Am. Chem. Soc. 136 (2014) 5237–5240.
[9] O.P. Singh, N. Vijayana, K.N. Sood, B.P. Singh, V.N. Singh, J. Alloys Compd. 648 (2015) 595–600.
[10] G. Wang, A.C.S. Appl. Mater. Interfaces 5 (2013) 10042–10047.
[11] W. Ki, H.W. Hillhouse, Adv. Energy Mater. 1 (2011) 732–735.
[12] J. Ge, S. Zuo, J. Jiang, J. Ma, L. Yang, P. Yang, J. Chu, Appl. Surf. Sci. 258 (2012) 7844–7848.
[13] G. Chen, C. Yuan, J. Liu, Z. Huang, S. Chen, We. Liu, G. Jiang, C. Zhu, J. Power Sources 276 (2015) 145–152.
[14] S. Chen, X.G. Gong, A. Walsh, S. Wei, Appl. Phys. Lett. 96 (2010) 021902.
[15] P. Prabeesh, P. Saritha, I. Packia Selvam, S.N. Potty, Mater. Res. Bull. 86 (2017) 295–301.
[16] D.H. Kuo, M. Tsega, Mater. Res. Bull. 49 (2014) 608–613.
[17] V. Tunuguntla, W.C. Chen, P.H. Shih, I. Shown, Y.R. Lin, J.S. Hwang, C.H. Lee, L.C. Chenc, K.H. Chen, J. Mater. Chem. A 3 (2015) 15324–15330.
[18] B. Long, S.Y. Cheng, Q. Zheng, J.L. Yu, H.J. Jia, Mater. Res. Bull. 73 (2016) 140–144.
[19] M. Grossberg, J. Krustok, J. Raudoja, K. Timmo, M. Altosaar, T. Raadik, Thin Solid Films 519 (2011) 7403–7406.
[20] G. Chen, J. Li, M. Wu, J. Liu, F. Lai, C.i Zhu, Mater. Lett. 159 (2015) 32–34.
[21] D.B. Mitzi, O. Gunawan, T.K. Todorov, K. Wang, S. Guha, Sol. Energy Mater Sol. Cells 95 (2011) 1421–1436.
[22] G. Chen, C. Yuan, J. Liu, Y. Deng, G. Jiang, W. Liu, C. Zhu, J. Power Sources 262 (2014) 201–206.
[23] S. Das, K.C. Mandal, Mater. Res. Bull. 57 (2014) 135–139.
[24] S. Jeong, B.S. Lee, S.J. Ahn, K.H. Yoon, Y.H. Seo, Y. Choi, B.H. Ryu, Energy Environ. Sci. 5 (2012) 7539–7542.
[25] R. Caballero, C. Maffiotteb, C. Guillén, Thin Solid Films 474 (2005) 70–76.
[26] O.P. Singh, N. Vijayan, K.N. Sood, B.P. Singh, V.N. Singh, J. Alloys Compd. 648 (2015) 595–600.
[27] H. Duan, W. Yang, B. Bob, C. Hsu, B. Lei, Y. Yang, Adv. Funct. Mater. (2013) 1466–1471.
[28] T. Gokmen, O. Gunawan, T.K. Todorov, D.B. Mitzi, Appl. Phys. Lett. 103 (2013) 103506.
[29] H. Xie, M. Dimitrievska, X. Fontané, Y. Sánchez, S. López-Marino, Izquierdo-Roca, V. Bermúdez, A. Pérez-Rodrígue, E. Saucedo, Sol. Energy Mater Sol. Cells 140 (2015) 289–298.
[30] J.R. Sites, P.H. Hauk, Sol. Cells 27 (1989) 411–417.